

Supporting information

Nanoparticles of lignin and saccharides from fishery wastes as sustainable UV-shielding, antioxidant and antimicrobial bio-fillers

Eliana Capecchi^{1,}, Elisabetta Tomaino¹, Davide Piccinino¹, Peter Elias Kidibule², Maria Fernández-Lobato², Daniele Spinelli³, Rebecca Pogni⁴, Ana Garcia Cabado⁵, Jorge Lago⁵, Raffaele Saladino^{1,*}.*

Supporting information S1 Production of Chit 33

Supporting information S2 DSC curves of KLNPs and OLNPs (Figure S2.1), CH/KNPs and CH/OLNPs (Figure S2.2), and COS/OLNPs (Figure S2.3), respectively.

Supporting information S3 FT-IR of original CH 1-7 (Panel A) and OL (Panel B)

Supporting information S4 Morphological analysis of CH/KNPs (Figure S4.1) and dimensional analysis of CH/KNPs (Table S4.2).

Supporting information S5 UV-absorbing spectra of CH/KNPs

Supporting information S6 Antimicrobial activity for CH/OLNPs and CH/KNPs

Supporting information S7 UV-visible absorption spectra of COS3/OLNPs and OLNPs (Panel A), and translation of the UV-visible absorption spectra into Tauc's plots to calculate the HOMO-LUMO gap of COS3/OLNPs and OLNPs

Supporting information S1 Production of Chit 33

The gene *chit33* from *Trichoderma harzianum* CECT2413 fused to the *Saccharomyces cerevisiae* MF1 secretion signal was previously cloned in plasmid pIB4 and expressed in *Pichia pastoris* as previously reported¹. The *P. pastoris* fermentation was obtained in a 5 L bioreactor (Biostart BPluss Sartorius Ltd., Gottingen, Germany) containing 3.5 L of medium (40 g/L glycerol, 26.7 mL H₃PO₄ 85%, 0.93 g/L CaSO₄, 18.2 g/L K₂SO₄, 14.9 g/L MgSO₄, 4.13 g/L KOH, 2 mL biotin (0.2 g/L), and 4.35 mL of PTM1 trace salts). The fermentation parameters were maintained at 30 °C, 600 rpm agitation, 20% dissolved oxygen and pH was controlled at 5.0 units with NH₄OH 28% (v/v) during 24 h (~40 OD₆₀₀ units). Then 100% methanol was added continuously during 4 days at 20 µL/min L of fermentation volume to induce the expression of protein Chit33 (final ~300 OD₆₀₀ units). Culture growth were monitored spectrophotometrically at 600 nm (OD₆₀₀) and protein concentration using NanoDrop at 280 nm. The cells were removed by centrifuging at 6000 × *g* for 15 min, then the extracellular fraction was concentrated using 10000 MWCO PES membranes in a Vivaflow 50 system (Sartorius, Gottingen, Germany).

Supporting information S2 DSC curves of KLNPs, and OLNPs (Figure S2.1), CH/KLNPs and CH/OLNPs (Figure S2.2) and COS/OLNPs (Figure S2.3), respectively.

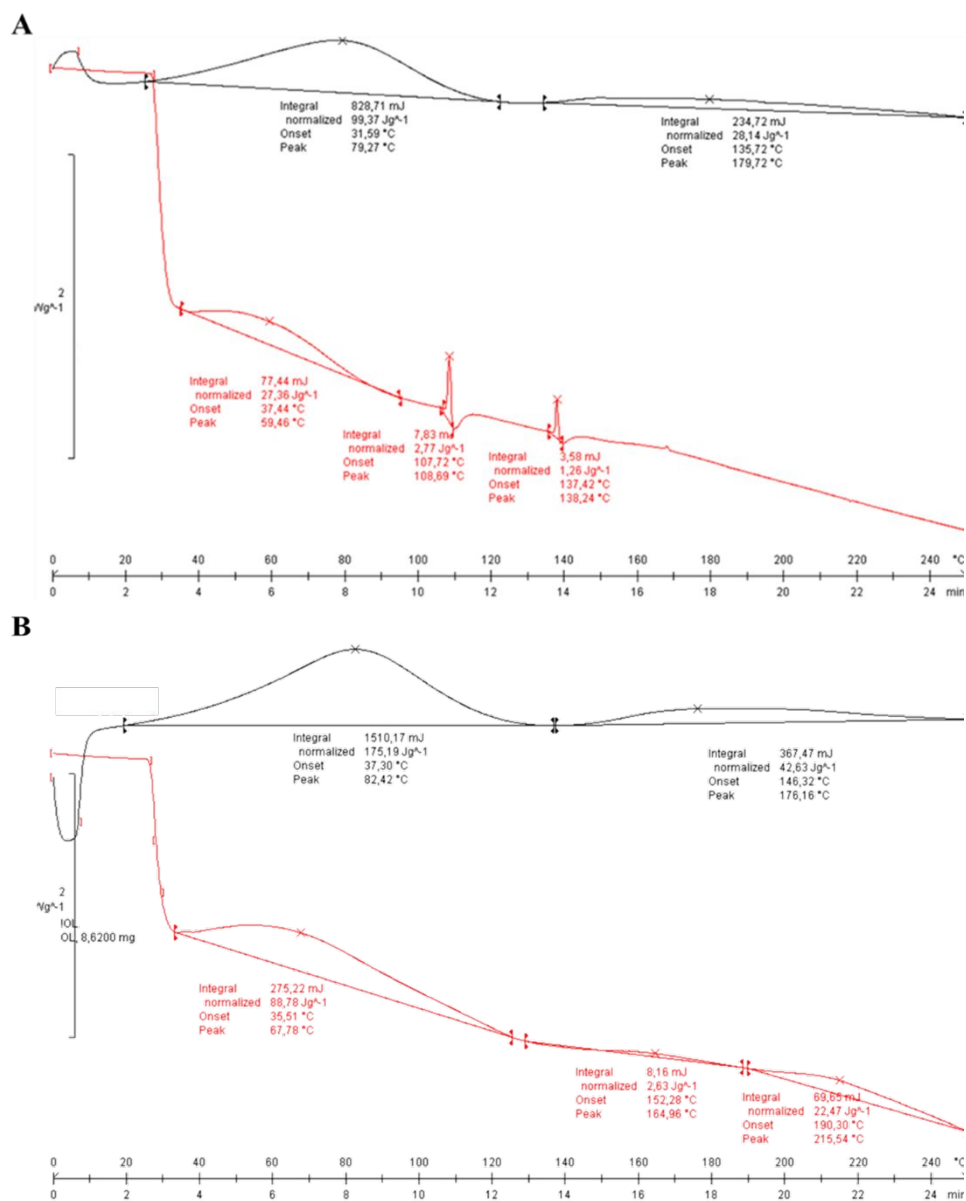


Figure S2.1 Panel A: DSC curves of KLNPs (red line) *versus* KL (black line). Panel B: DSC curves of OLNPs (red line) *versus* OL (black line).

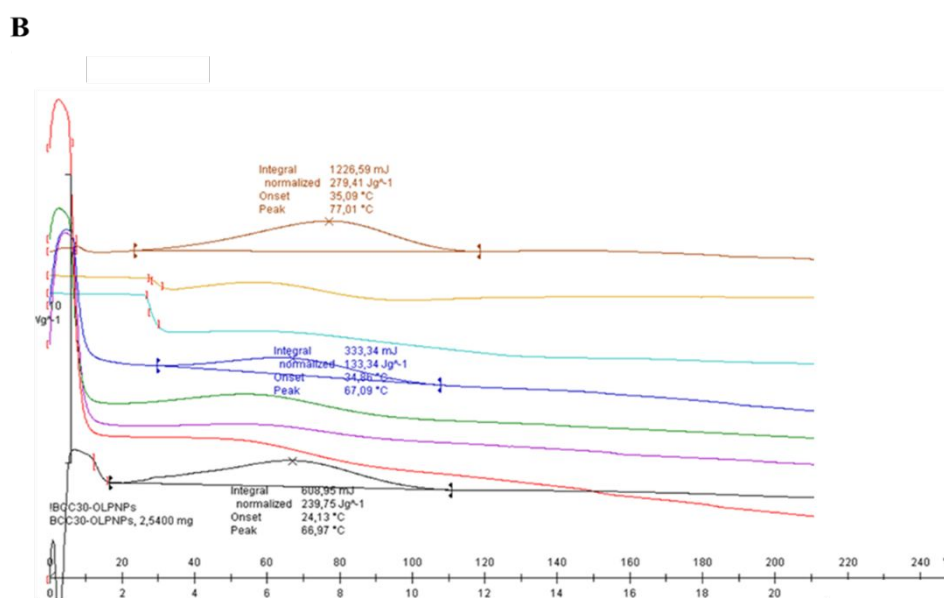
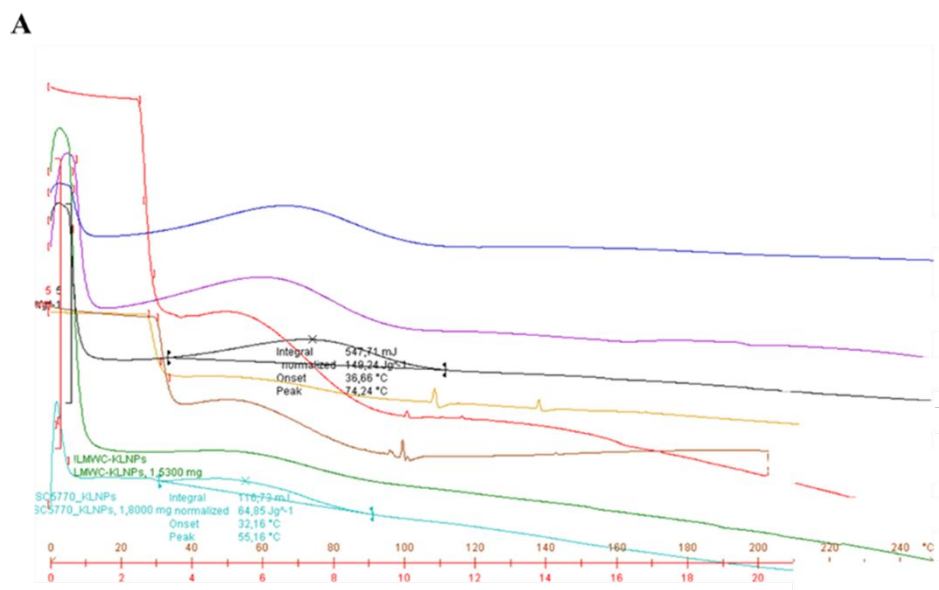
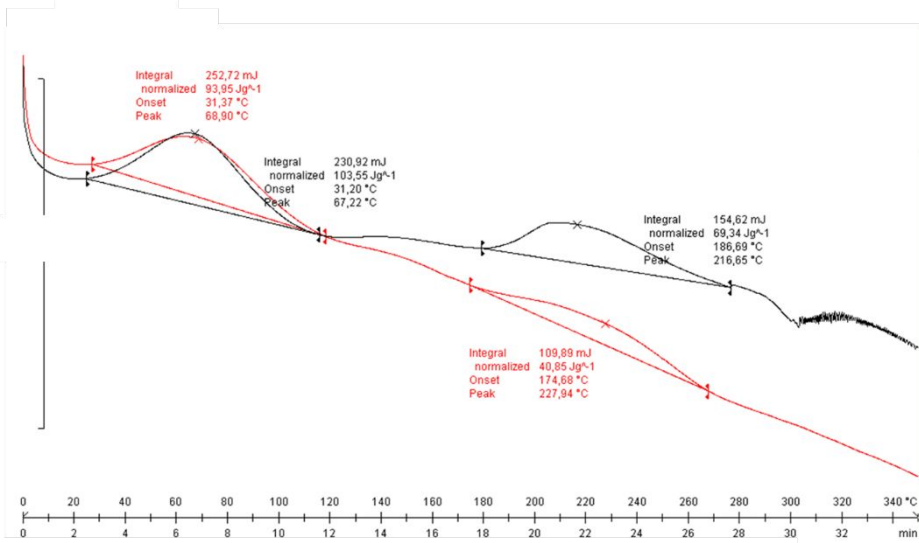
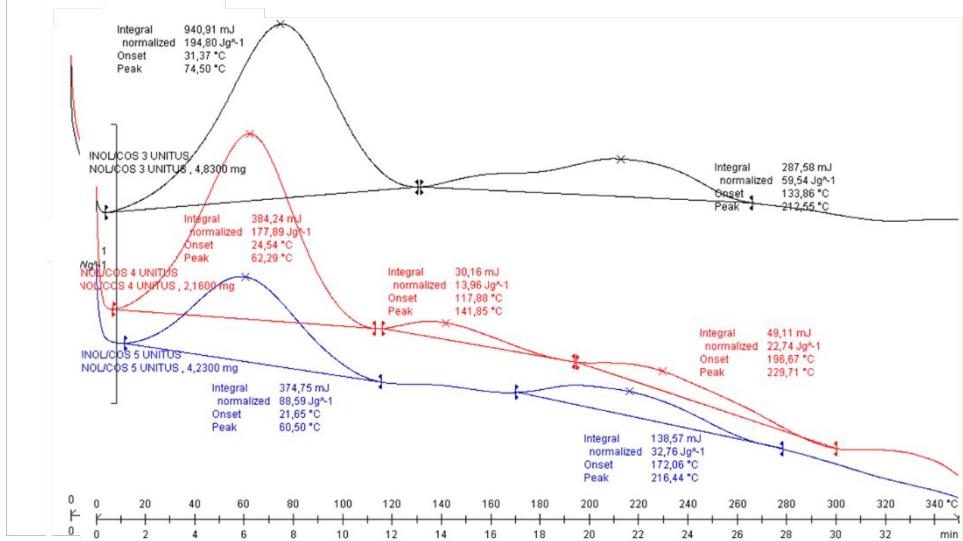
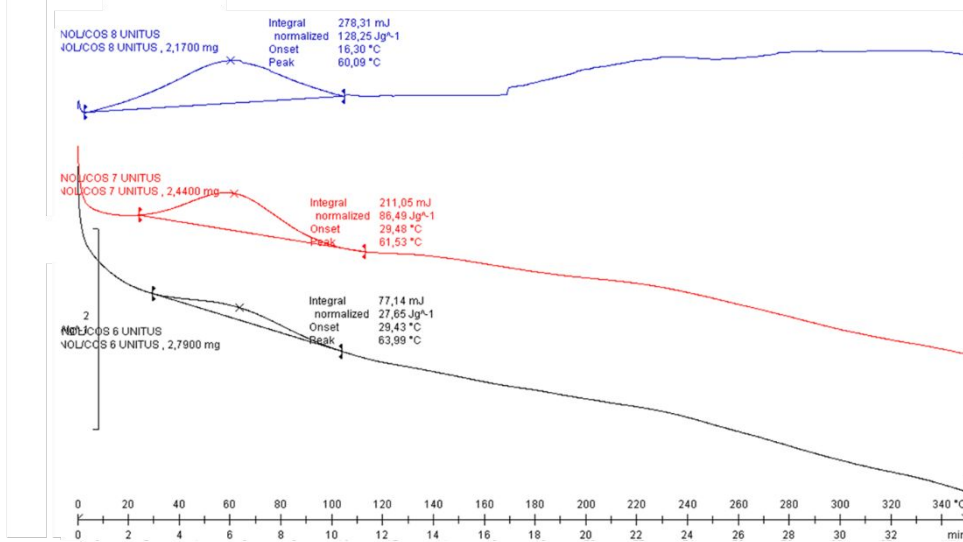


Figure S2.2 Panel A: DSC curves of **CH/KLNPs** versus KLNPs assigned with the following color code: KLNPs (yellow line), **CH1/KLNPs** (brown line), **CH2/KLNPs** (azure line), **CH3/KLNPs** (red line), **CH4/KLNPs** (black line), **CH5/KLNPs** (purple line), **CH6/KLNPs** (green line), **CH7/KLNPs** (blue line). Panel B: DSC curves of **CH/OLNPs** versus OLNPs assigned with the following color code: OLNPs (azure line), **CH1/OLNPs** (brown line), **CH2/KLNPs** (yellow line), **CH3/KLNPs** (red line), **CH4/KLNPs** (black line), **CH5/KLNPs** (purple line), **CH6/KLNPs** (green line), **CH7/KLNPs** (blue line).

A**B****C**

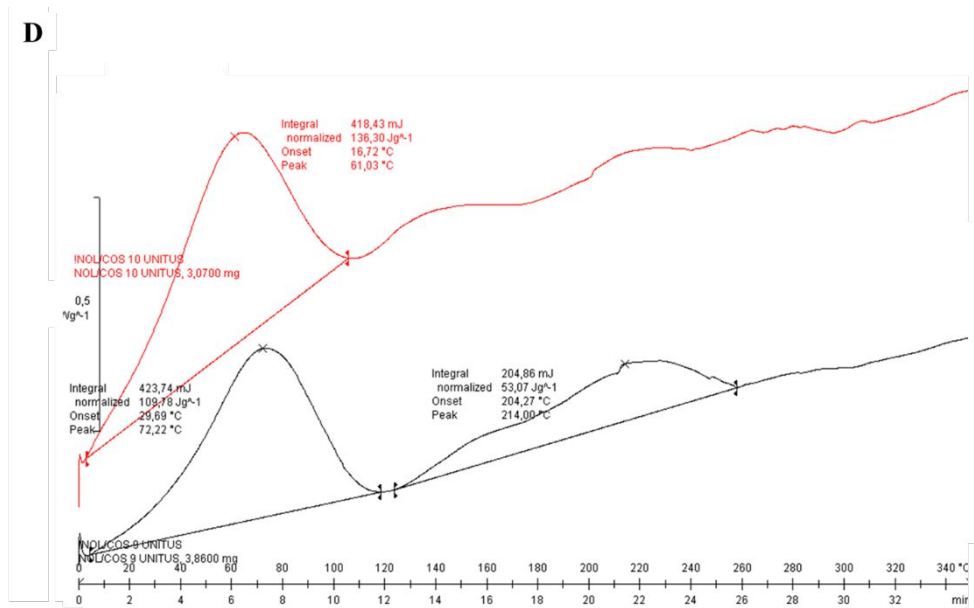
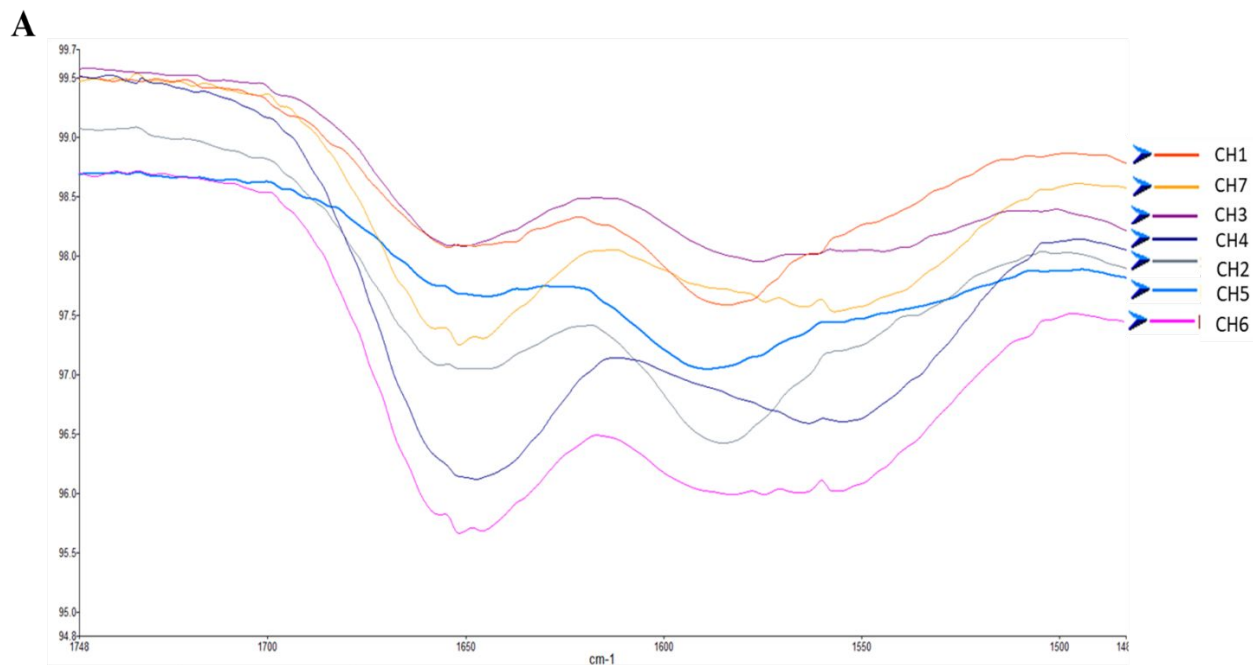


Figure S2.3 Panel A: DSC curves of **COS1/OLNPs** (black line) and **COS2/OLNPs** (red line). Panel B: DSC curves of **COS3/OLNPs** (black line), **COS4/OLNPs** (red line) and **COS5/OLNPs** (blue line). Panel C: DSC curves of **COS6/OLNPs** (black line), **COS7/OLNPs** (red line) and **COS8/OLNPs** (blue line). Panel D: DSC curves of **COS9/OLNPs** (black line) and **COS10/OLNPs** (red line).

Supporting information S3 FT-IR of original CH 1-7 (Panel A) and OL (Panel B)



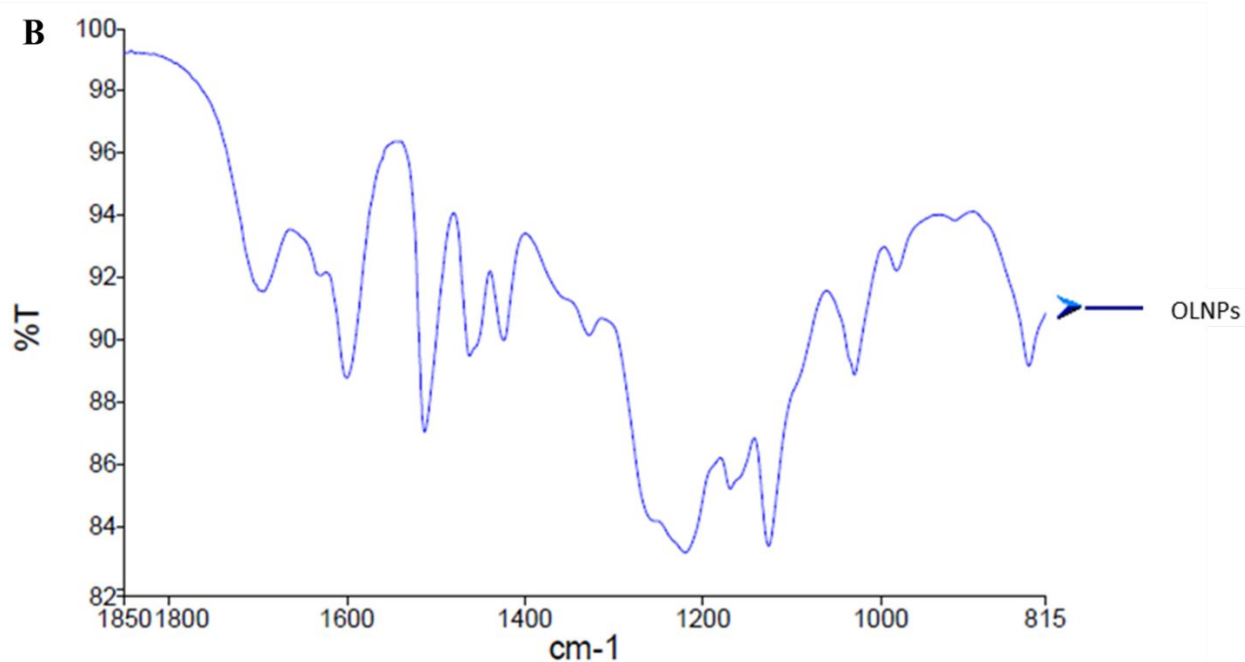


Figure S3. FT-IR spectra of original CH 1-7 and OL. Panel A: amide I band (1649 cm⁻¹) and amide II band (1585 cm⁻¹) of CH. Panel B: 1614 cm⁻¹ (C=C Aromatic bending vibration), 1462 cm⁻¹ (C-H deformations in -CH₂- and -CH₃ vibration band), 1332 cm⁻¹ (C=O stretching of syringyl unit), and 1116 cm⁻¹ (aromatic C-H in plane deformation of syringyl unit), respectively.

Supporting information S4 Morphological analysis of CH/KLNPs (Figure S4.1) and dimensional analysis of CH/KLNPs (Table S4.2).

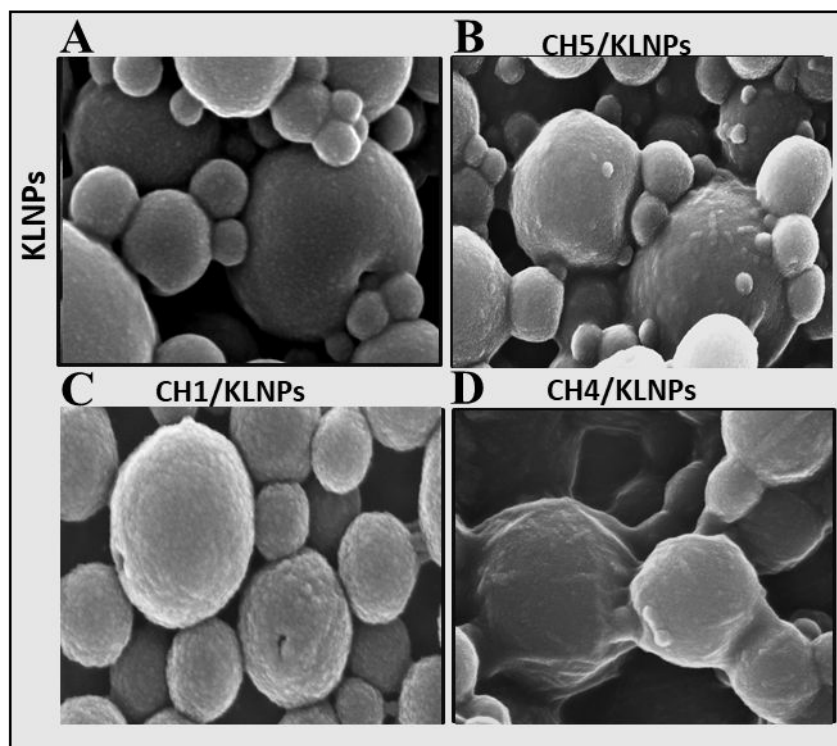


Figure S4.1. SEM images of **CH/KLNPs**. Panel A: **CH/KLNPs** bearing CH with high DD (**CH5/KLNPs** and **CH1/KLNPs**) and low DD (**CH4/KLNPs**), respectively.

Table S4.2 DLS and ζ -potential of **CH/OLNPs** and **COS/OLNPs**

Entry	Sample	Size(nm)	PDI ^a	ζ -Potential (mV)
1	KLNPs	210	0,35	-42
2	CH1/KLNPs	586	0,40	+69
3	CH4/KLNPs	551	0,54	+50
4	CH5/KLNPs	160	0,23	+30

^aPolydispersion index.

Supporting information S5 UV-absorbing spectra of **CH/KLNPs**

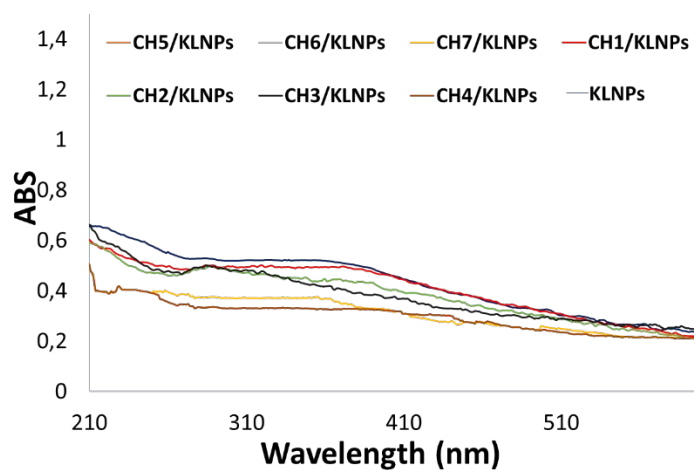


Figure S5. UV-absorbing capacity of **CH/KLNPs**

Supporting information S6 Antimicrobial activity of **CH/OLNPs** and **CH/KLNPs**

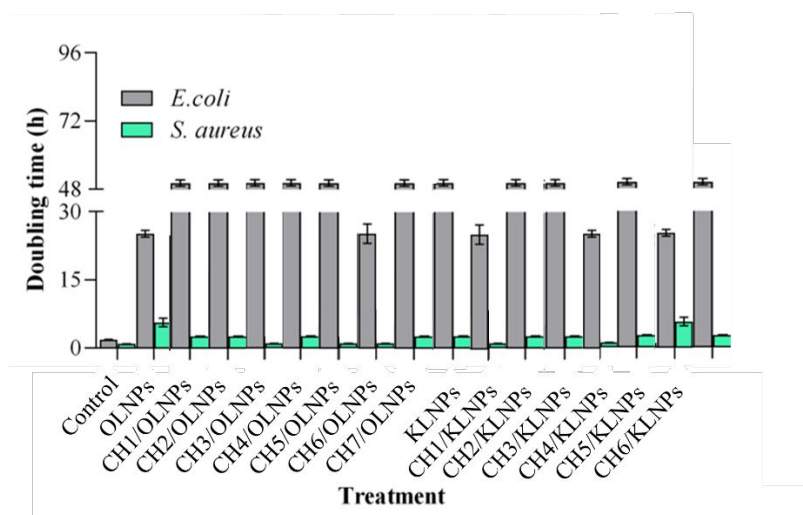
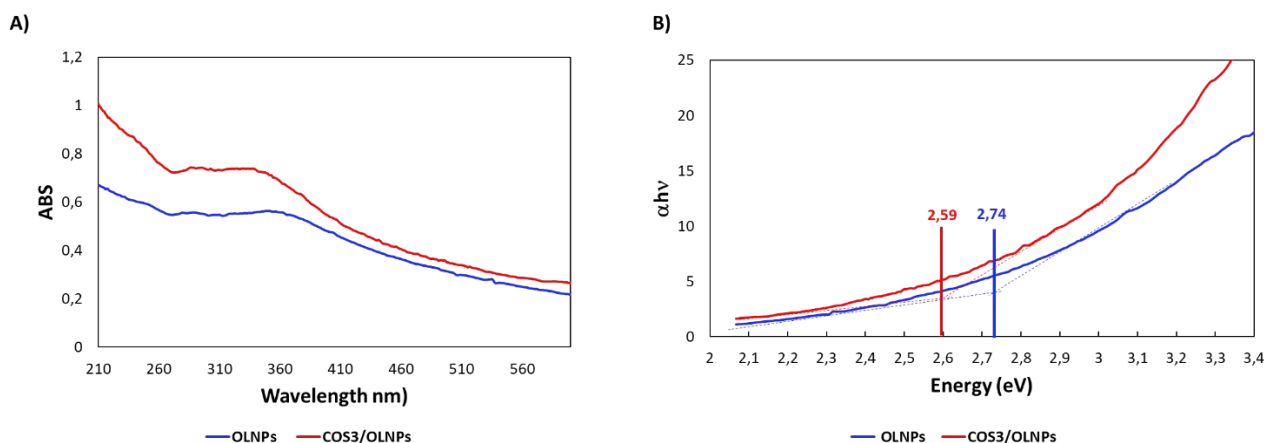


Figure S6. The doubling time for the referred Gram-negative and Gram-positive bacteria of CH/OLNPs and CH/KLNPs

Supporting information S7 UV-visible absorption spectra of **COS3/OLNPs**, and OLNPs (Panel A)

and translation of the the UV-visible absorption spectra into Tauc's plots to calculate the HOMO-

LUMO gap of **COS3/OLNPs**, and OLNPs



1. Kidibule, P. E.; Santos-Moriano, P.; Plou, F. J.; Fernández-Lobato, M. Endo-chitinase Chit33 specificity on different chitinolytic materials allows the production of unexplored chito oligosaccharides with antioxidant activity. *J. Appl. Biotechnol. Rep.*, 2020, 27, 500.

